

Spectroscopy of Optically Selected BL Lac Objects and their γ -ray emission

A. Sandrinelli

Università degli Studi dell'Insubria, Via Valleggio 11, I-22100 Como, Italy

INAF - Osservatorio Astronomico di Brera, Via Emilio Bianchi 46, I-23807 Merate, Italy

INFN - Istituto Nazionale di Fisica Nucleare

`angela.sandrinelli@brera.inaf.it`

A. Treves

Università degli Studi dell'Insubria, Via Valleggio 11, I-22100 Como, Italy

INAF - Istituto Nazionale di Astrofisica

INFN - Istituto Nazionale di Fisica Nucleare

R. Falomo

INAF - Osservatorio Astronomico di Padova, Vicolo dell Osservatorio 5, I-35122 Padova, Italy

E. P. Farina

Università degli Studi dell'Insubria, Via Valleggio 11, I-22100 Como, Italy

INFN - Istituto Nazionale di Fisica Nucleare

L. Foschini

INAF - Osservatorio Astronomico di Brera, Via Emilio Bianchi 46, I-23807 Merate, Italy

M. Landoni

Università degli Studi dell'Insubria, Via Valleggio 11, I-22100 Como, Italy

INAF - Osservatorio Astronomico di Brera, Via Emilio Bianchi 46, I-23807 Merate, Italy

INFN - Istituto Nazionale di Fisica Nucleare

– 2 –

and

B. Sbarufatti

INAF - Osservatorio Astronomico di Brera, Via Emilio Bianchi 46, I-23807 Merate, Italy
Pennsylvania State University, Department of Astronomy and Astrophysics, PA 16801,
USA

Received _____; accepted _____

ABSTRACT

We present Very Large Telescope optical spectroscopy¹ of nine BL Lac objects of unknown redshift belonging to the list of optically selected radio loud BL Lacs candidates. We explore their spectroscopic properties and the possible link with gamma ray emission. From the new observations we determine the redshift of four objects from faint emission lines or from absorption features of the host galaxy. In three cases we find narrow intervening absorptions from which a lower limit to the redshift is inferred. For the remaining two featureless sources, lower limits to the redshift are deduced from the very absence of spectral lines. A search for γ counterpart emission shows that six out of nine are *Fermi* γ -ray emitters with two new detections. Our analysis suggests that most of the BL Lac still lacking of redshift information are most probably located at high redshift.

Subject headings: BL Lacertae objects: general, Galaxies: distances and redshifts.

¹Based on observations made with ESO Telescopes at the Paranal Observatory under program 083.B-0187(A).

1. Introduction

BL Lac objects are active galactic nuclei (AGNs) characterized by strong and rapid flux variability, polarization, and weakness or absence of spectral emission lines. With the flat spectrum radio quasars (FSRQ), BL Lacs represent a type of radio loud objects called blazars. As proposed in the seminal paper of Blandford & Rees (1978), blazars are AGNs with relativistic jets pointing close to the direction of the observer. They are the dominant population of the extragalactic γ -ray sky both at GeV and TeV energies. At radio frequencies, BL Lacs display strong core compact flat spectrum emissions. In the optical range, synchrotron continuum is boosted by relativistic beaming resulting in a depression of the equivalent width of the spectral lines, especially in the high states spectra, making often the detection of the redshift a challenging task and a central issue in γ astronomy.

The first complete surveys of BL Lac objects were performed in the radio band considering as distinguish feature the flatness of the radio spectrum (e.g. Stickel et al. 1991). In X-rays the BL Lac surveys were a sub-product of "complete" sky surveys (see e.g. Stocke et al. 1985, 1991). The Palomar Green survey (Green et al. 1986), aimed to build a complete list of quasars through their colors, gave four bright BL Lacs. The optical spectroscopy was consequent, since the commonly used criterion for defining a BL Lac is the line equivalent widths $EW < 5 \text{ \AA}$ (e.g. Marcha et al. 1996). The detection of these weak features requires spectroscopy of adequate spectral resolution and signal to noise. Observations with medium aperture telescopes provided the redshift of a number of BL Lacs (e.g., Falomo et al. 1987b,a; Ulrich 1989; Falomo 1990; Stickel et al. 1993; Veron 1994; Marcha et al. 1996; Carangelo et al. 2003) but for many of them, in particular those with a strong nuclear component, the redshift remained unknown. With 8m class telescopes the situation improved as demonstrated, among the recent systematic spectroscopic campaigns, by our study of 69 BL Lacs in the southern sky with ESO-VLT+FOR2,

which yielded 23 new redshifts of BL Lacs basically selected in the Giommi/Padovani list (Padovani & Giommi 1995) before the *Fermi* launch (Sbarufatti et al. 2005a,b, 2006a,b, 2009, Landoni et al. 2013; spectra and redshifts are available in electronic form in our website <http://www.oapd.inaf.it/zbl lac/>).

In the last decade in parallel with the activity related to the high energy emission, a substantial progress in discovering new BL Lacs and their redshift derived from large optical spectroscopic surveys, in combination with radio and X-ray catalogs. Plotkin et al. (2008; hereafter P08) selected 501 BL Lacs candidates combining the Faint Images of the Radio Sky at Twenty-Centimeters (FIRST, Becker et al. 1995) radio survey with the Sloan Digital Sky Survey Data Release 5 (SDSS DR5) spectroscopic data base, under the conditions of featureless or weak features spectra and Ca II H/K depression less than 40%. A substantial fraction of sources, ($\sim 60\%$) lacks of reliable spectroscopic redshifts. Recently, Shaw et al. (2013; hereafter S13) using different telescopes, produced spectra of most of the *Fermi* 475 BL Lac candidates (Ackermann et al. 2011), obtaining redshifts for $\sim 44\%$ of the sample and constraining z for nearly all remaining objects. However, in order to characterize the general properties of the BL Lac population it is highly desirable to define an homogeneous sample of BL Lacs not biased by the properties introduced in the selection by the X-rays and radio surveys. For instance, Collinge et al. (2005) compiled a large optically selected sample (386 targets) from 2860 deg² of the SDSS, chosen to have quasi-featureless optical spectra and low proper motions. Some radio-quiet sources were found, almost all without X-ray counterparts in ROSAT All-Sky Survey (RASS; Voges et al. 1999). Plotkin et al. (2010a; hereafter P10) expanded the Collinge sample through a complex sieving procedure of SDSS DR7 (Abazajian et al. 2009), and recovered 723 purely optically selected BL Lacs, included a fraction of 86 radio-quiet objects, the majority of which are unlikely *bona fide* BL Lacs, but rather a distinct class of quasars with intrinsically weak emission lines (Plotkin et al. 2010b, Wu et al. 2012). Approximately $\sim 80\%$ of the whole P10 sample

match to a radio source in FIRST/NRAO VLA Sky Survey (NVSS; Condon et al. 1998), and $\sim 40\%$ match to a RASS X-ray source. Spectroscopic redshifts are given for $\sim 36\%$ of the radio-loud subsample.

For this elusive class of objects the adopted selection criteria can affect the redshift distributions of the BL Lacs and cause different cosmological evolution scenarios, see e.g. the discussions in Bade et al. (1998) and in Giommi et al. (2012). Radio selected BL Lacs seem to display a positive evolution (i.e. the number density or the luminosity shows a decrease with cosmic time), while for X-ray selected objects a negative one was proposed, or not evolution at all (Rector et al. 2000, Rector & Stocke 2001, Caccianiga et al. 2002, Beckmann et al. 2003, Padovani et al. 2007, Ajello et al. 2009, Giommi et al. 2009, 2012 and references therein). A continuum trend from slightly positive-evolution low peaked BL Lacs to strong negative-evolution high peaked was proposed (Rector et al. 2000), also related to their X-ray to radio flux ratio (Giommi et al. 1999, 2012). Statistics concerning the evolution of the BL Lacs suffer of redshift incompleteness, making the increase of the objects with reliable redshifts from homogeneous and unbiased selections a core issue (see also Shaw et al. 2013 for a discussion).

In this paper we present optical spectroscopy of a small sample (9 targets) of BL Lacs of still unknown redshift belonging to the P08 catalog of radio selected BL Lacs. We note that our sample is also entirely included into P10 catalog of optically selected BL Lacs. We describe our observations and analysis of spectra in section 2 together with the new redshifts; then we search for the counterparts in the *Fermi* Gamma-ray Space Telescope archives (section 3). Summary and conclusions are given in section 4.

Throughout the paper we adopt the following concordant cosmology: $H_0 = 70 \text{ km s}^{-1} \text{ Mpc}^{-1}$, $\Omega_m = 0.30$ and $\Omega_\Lambda = 0.70$.

2. Optical Spectroscopy

2.1. Sample observations and data analysis

Within about 200 P08 BL Lacs objects with unknown redshift, we selected a small sample of 15 with the only requests that they were relatively bright objects ($r < 19.4$), well observable from Paranal (Chile) ESO premises and classified as high confidence BL Lacs. We stress that these are also all included in the P10 radio loud BL Lac candidates, selected on the only basis of their optical properties, thus we can consider them as *a posteriori* optically selected. We collected optical spectra of only 9 sources (see Table 1) out of 15 because of weather conditions.

Spectra were gathered with the FORS2 mounted on the Antu VLT of the ESO in Paranal. Observations were performed with the grism 300V and the 2'' width slit, yielding a spectral resolution at the central wavelength of $R = \lambda/\Delta\lambda \sim 350$ and covering 3800 – 8200 Å spectral range, and exploiting the better S/N ratio of VLT. The seeing in the nights of observations ranged from 0''.5 to 1''.2, with an average of $\sim 0''.9$, as reported in Table 1. Standard IRAF² tools were used in data reduction. We adopted the same procedures described in previous works (e.g. Sbarufatti et al. 2005a,b), including bias subtraction and flat fielding. For each target we obtained three or six individual spectra to make corrections for the cosmic rays and provide independent check of each signature, with typical total exposure times of 45 or 90 min respectively (see Table 1). Individual spectral frames are combined together taking the median, from which a one-dimensional spectrum is extracted. The wavelength calibration was achieved using the spectra of a Helium Neon Argon

²IRAF (Tody 1986) is distributed by the National Optical Astronomy Observatories, which are operated by the Association of Universities for Research in Astronomy, Inc., under co-operative agreement with the National Science Foundation.

lamp and typical uncertainties are $\sim 1 \text{ \AA}$. Spectra are corrected for Galactic reddening according with the Schlegel, Finkbeiner, & Davis (1998) maps and assuming $R_V = 3.1$ (e.g. Cardelli, Clayton, & Mathis 1989).

2.2. The optical spectra

The extracted spectra and the normalized spectra with respect to the continuum are reported both in Figure 1 and in electronic form in our mentioned website. For each spectrum the S/N is given in Table 1. The continuum was fitted with a power law, defined as $F_\lambda \propto \lambda^{-\alpha_\lambda}$. The resulting optical spectral indices are given in the Table 2 as α_ν ($F_\nu \propto \nu^{-\alpha_\nu}$, where $\alpha_\nu = 2 - \alpha_\lambda$) for consistency and easy comparison with the bulk of the literature. We find $0.73 < \alpha_\nu < 1.44$ corresponding to average value $\alpha_{\nu \text{ ave}} = 1.17$, both consistent with the average spectral index $\alpha_\nu = 1.15$ and the dispersion of 0.69 reported by P10.

In order to search for very weak spectral lines, we evaluated the minimum observable equivalent width (EW_{min}). Dividing the spectrum in 25 \AA bins, as fully described in Sbarufatti et al. (2005b), we objectively define the EW_{min} as twice the rms of the distribution of all the observer-frame EW s measured in each bin. The absorption and emission features with EW greater than this threshold are carefully inspected. ID labels mark the successful identifications in Figure 1 and in Table 2, where also EW_{min} and line properties are reported. For four sources we were able to obtain a redshift from the detection absorption/emission lines associated to the BL Lac host galaxy. In three cases, we observed absorption intervening features that, interpreted as Mg II 2800, allow us to set a lower limit to the redshift. In two cases the spectrum is featureless, thus we calculated a lower limit on z using the method described by Sbarufatti et al. (2005b, 2006a). Briefly, recalling that non thermal jet and the host galaxy both contribute to the observed flux

and assuming that BL Lac host galaxies are giant elliptical with $M_R^{host} = -22.90 \pm 0.50$ and standard absorption lines, one can infer a z dependent relationship between observed EW and emitted $EW_{rest} = EW/(1+z)$ equivalent widths. The absence of lines places $EW < EW_{min}$, providing a lower limit for z . In Table 2 we also report the redshift upper limit from the lack of the $Ly\alpha$ absorptions as $z_{upper} = \lambda_{lim}/1216 \text{ \AA} - 1 + \Delta z$, where Δz derives from the probability of not detection absorbers close to the blue limit wavelength λ_{lim} of the spectrum, taking into account the redshift dependence of $Ly\alpha$ forest absorbers density and its EW scaling (see Shaw et al. 2013 and references therein).

In the following we report further information on single sources.

2.3. Notes on individual sources.

J003808.50+001336.5: The spectrum shows a feature at $\lambda = 4780 \text{ \AA}$. We ascribed to Mg II $\lambda 2798$ intervening system absorption, which places the source at $z > 0.708$. This feature is, however, only detected at 2σ level. We also note that Mg II doublet is unresolvable with our observations. To complement our observations we retrieved all the spectra from the SDSS. This target was observed 3 times from MJD 51793 to 55444 with $S/N \sim 10$ and no reliable redshift is available.

J125032.58+021632.1: Mg II $\lambda 2798$ and O II $\lambda 3727$ emission lines are apparent, securing the source at $z = 0.995$. A tentative redshift of 0.953, warning flagged for multiple equal χ^2 best fits, was assigned to the source by the redshift fitting procedure in the SDSS DR9 based on a spectrum of $S/N \sim 10$, where the Mg II feature is loosely visible and detectable. For this optically selected BL Lac candidate the rest frame Mg II equivalent width is $EW_{rest} = 6.1 \pm 0.4 \text{ \AA}$, which makes marginal its inclusion in

the BL Lacs class. To evaluate a more physical discriminant parameter, the optical beaming factor δ , as discussed by Farina et al. (2012) and Landoni et al. (2013), was calculated. This parameter quantifies the contribution of thermal disk to the total luminosity (Decarli et al. 2011). A $\delta = 6.0 \pm 3.6$ places the source as a BL Lac just above the intermediate region between pure QSO ($\delta \simeq 1$) and BL Lacs ($\delta \gtrsim 4$) (Landoni et al. 2013).

J135120.84+111453.0: An absorption feature at $\lambda = 4530 \text{ \AA}$ is detected. If the interpretation is in terms of an Mg II $\lambda 2798$ intervening system, a redshift lower limit is 0.619. This absorption feature at $\lambda = 4530 \text{ \AA}$ was recently observed also by Shaw et al. (2013).

J144052.93+061016.1: Our spectrum exhibits Ca II H/K $\lambda\lambda 3934, 3968$ and G Band $\lambda 4305$ absorptions lines from underlying host galaxy at $z = 0.396$. Two optical spectra are gathered by SDSS on MJD 53494 and 55686 and inferred redshifts are given as unreliable. Shaw et al. (2013) detected an absorption feature $\lambda \sim 3685 \text{ \AA}$, that interpreted as Mg II set a lower limit at 0.316.

J163716.73+131438.7: In our spectrum we detect a narrow emission line at $\lambda = 6170 \text{ \AA}$. This is most probably a real feature, since it clearly appears on each of the three individual spectra. It can be identified with O II $\lambda 2737$ at $z = 0.656$. At the same redshift two absorption lines ascribed to Ca II H/K $\lambda\lambda 3934, 3968$ are apparent. In addition, the position of an absorption at $\lambda = 7124 \text{ \AA}$, encompassed by two H₂O telluric bands, is consistent with G band absorption at the same redshift of the other lines. Our redshift is one of the highest ever been detected in optical range by host galaxy absorption lines.

J214406.27-002858.1: Because of the featureless spectrum, a redshift lower limit of ~ 0.34 is derived from $EW_{min} = 1.36 \text{ \AA}$. Unreliable redshifts were assigned by the SDSS.

J224448.09-000619.3: We clearly detected Ca II H/K $\lambda\lambda 3934, 3968$ absorptions at redshift $z = 0.641$. The position of an absorption at $\lambda = 7057 \text{ \AA}$ in a region inside the H₂O telluric bands, is consistent with G band $\lambda 4305$ absorption at the same redshift of Ca II doublet wavelengths. No reliable redshift was obtained by the SDSS.

J224730.18+000006.4: We distinctly observed an absorption feature at $\lambda = 5311 \text{ \AA}$ with an $EW = +3.0 \pm 0.1 \text{ \AA}$, that was interpreted as Mg II $\lambda 2798$ intervening system setting $z > 0.898$. There is no evidence of the emission line feature detected by Shaw et al. (2013) at $\lambda \sim 5460 \text{ \AA}$ and taken as Mg II at $z = 0.949$. We suspect this feature to be instrumental since it appears in other spectra reported by Shaw with the same spectrograph.

3. High Energy Emission of the Sources

The *Fermi* Second Source Catalog (2LAC, Nolan et al. 2012) lists the 1873 significant sources detected by the Large Area Telescope (LAT, Atwood et al. 2009) during *Fermi*'s first two years of sky survey observations. Most of them are jet dominated AGN. Among them, more than 400 *Fermi* BL Lacs attest about their large contribution to the γ emission background among the brightest extra-Galactic sources. To fully describe our small sample of optically selected BL Lacs, the detections of the target objects at high and very high energy were investigated. A comparison with TevCat³ (Horan & Wakely 2008) indicates that there are no TeV counterparts. This is not surprising, since measured redshifts or a

³<http://tevcat.uchicago.edu/>

lower limits to the redshift are beyond the extragalactic background light horizon, with the exception of J144052.93+061016.1.

We have cross-correlated the *Fermi* archived events available on line⁴ with the positions of our sources to update with respect to LAT 2 release. As shown in Table 3, four of our sources enter in the 2LAC catalogue (LAT AGN Catalog, Ackermann et al. 2011). Then, we have analyzed all the available 57 month survey data, from the start of the *Fermi* activity on 2008 August 4 (MJD 54682) to 2013 April 8 (MJD 56390), with the aim of updating the values of flux and photon index, tracing the light curves and looking for new detections. We used the LAT Science Tools v. 9.27.1, the Instrument Response Function (IRF) P7SOURCE_V6, the corresponding background files, following standard procedures⁵. We selected for each source all the events of class 2 (“source” type) included in a circular region centered on the optical coordinates and with radius 10°. The final source list was determined, by applying a significance threshold.

Two new γ -ray sources appear: J125032.58+021632.1 and J163716.73+131438.8. Some targets, even if included in 2LAC, have not been detected on the basis on their γ fluxes over the entire 57 months period, but due to the variability they are found on monthly scale. In Table 3 the integrated photon flux in 0.1-100 GeV range or upper limits, the photon index and Test Statistic (TS, Mattox et al. 1996) are given for the whole time of observation in the central columns, while the right columns refer to monthly detections with highest TS. We considered as valid the results of the likelihood with $TS \geq 9$, corresponding to about 3σ .

In order to compare these results with the whole dataset, we have correlated the list

⁴http://fermi.gsfc.nasa.gov/ssc/data/access/lat/2yr_catalog/

⁵<http://fermi.gsfc.nasa.gov/ssc/data/analysis/scitools/>

of 637 radio loud optically selected BL Lacs of P10 with 2LAC, finding 125 positional coincidences, corresponding to ~ 20 % of the objects. In the sample examined here we observed a higher percentage, possibly as a consequence of the imposed magnitude limit, and the choice of SDSS lineless objects, which can be indicative of strong beaming. We have therefore selected the 194 P10 objects which are lineless and with $r < 19.4$, and found 69 correlations with 2LAC, corresponding to ~ 35 %, which is consistent with our findings.

4. Summary and Conclusions

We obtained optical spectroscopy of a small sample of BL Lacs of unknown redshift. On the basis of the γ properties the objects appear representative of the parent sample. In one case a broad line emission was found, in others absorptions from the host galaxy or intervening material were detected. For two objects the spectrum remained featureless, and in these cases the redshift should be $z \gtrsim 0.4$. New surveys have allowed to derive the spectroscopic redshifts of a large number of BL Lac objects with high S/N spectra. Nevertheless a significant fraction remains of unknown z objects. The new redshifts are higher compared to the ones of recently assembled large samples (P08, P10, S13). If tentative attributions and lower limits are included, redshift medians for high confidence BL Lacs are 0.39 in P08, 0.43 in P10 radio-loud subsample, 0.32 in S13 and 0.64 for our objects. Although it is a small sample, it suggests that a significant fraction of most still unknown z objects is probably at high z and significantly beamed. Larger redshift completeness fraction and homogeneous and unbiased selections could also better define a deeper picture of the cosmological evolution. A search for γ counterpart emission shows that six out of nine are Fermi γ -ray emitters with two new detections. High z and high beamed BL Lacs deserve new approach and capabilities to derive their redshifts. In the region of $z \sim 0.1 - 0.7$ a very effective technique was introduced in the far-UV (1135 – 1800

Å) with HST+COS (e.g. Stocke et al. 2011, Danforth et al. 2010, 2013), for constraining quite stringently z by intervening intergalactic medium absorbers detected in $Ly\alpha$, and in $Ly\beta$ and/or metal lines. An interesting possibility is derive z lower limits for BL Lacs objects at redshift $z > 1.5$ by searching for weak and narrow $Ly\alpha$ absorption in optical range from the ground similarly as performed and adopted in UV spectra. Good candidates can be found also in the sample presented here. High resolution spectroscopy is required combined with large diameter telescopes.

Table 1: Journal of observations.

Source	R.A.	DEC.	Date	r	Exp.Time	N	Seeing	S/N
	[h:m:s]	[d:m:s]		[mag]	[min]		[arcsec]	
(a)	(b)	(c)	(d)	(e)	(f)	(g)	(h)	(i)
J003808.50+001336.5	00 38 08.503	+ 00 13 36.53	2009-06-13	19.30	90	6	0.6	50
J125032.58+021632.1	12 50 32.581	+ 02 16 32.173	2009-04-30	19.22	45	3	0.9	30
J135120.84+111453.0	13 51 20.847	+ 11 14 53.02	2009-06-24	18.58	45	3	1.0	100
J144052.93+061016.1	14 40 52.94	+ 06 10 16.2	2009-06-24	17.17	45	3	1.1	140
J145507.44+025040.2	14 55 07.443	+ 02 50 40.25	2009-08-12	19.40	45	3	0.7	35
J163716.73+131438.8	16 37 16.737	+ 13 14 38.80	2009-04-29	18.95	45	3	1.2	90
J214406.27-002858.1	21 44 06.271	– 00 28 58.19	2009-05-19	19.20	45	3	0.7	15
J224448.09-000619.3	22 44 48.095	– 00 06 19.49	2009-08-15	19.11	45	3	0.5	90
J224730.19+000006.4	22 47 30.196	+ 00 00 06.463	2009-09-09	18.26	45	3	1.1	45

Note. — (a) Object ID. (b),(c) ICRS Right ascension and Declination Coordinates (J2000). (d) Date of observation. (e) r apparent PSF magnitude from SDSS DR7. (f) Total exposure time. (g) Number of collected spectra. (h) Seeing during the observation. (i) Signal to noise ratio evaluated as the average over the whole spectrum range, avoiding the regions affected by emission or absorption features.

Table 2: Spectral Line Parameters

Source	z	α_ν	EW_{min} [Å]	Line ID	λ_{line} [Å]	Type	FWHM [km/s]	EW [Å]
(a)	(b)	(c)	(d)	(e)	(f)	(g)	(h)	(i)
J003808.50+001336.5	$0.708 < z \lesssim 2.7$	1.14	0.78	Mg II	4780	a	900 ± 200	$+1.6 \pm 0.3$
J125032.58+021632.1	0.955	1.44	1.05	Mg II	5469	e	4500 ± 200	-12.1 ± 0.8
				O II	7288	e	700 ± 200	-3.6 ± 0.8
J135120.84+111453.0	$0.619 < z \lesssim 2.4$	0.73	0.31	Mg II	4530	a	1500 ± 300	$+1.0 \pm 0.2$
J144052.93+061016.1	0.396	1.08	0.28	Ca II	5491	g	1500 ± 600	$+0.4 \pm 0.1$
				Ca II	5542	g	1000 ± 200	$+0.4 \pm 0.1$
				G band	6008	g	1750 ± 50	$+0.93 \pm 0.04$
J145507.44+025040.3	$0.47 < z \lesssim 2.5$	1.44	0.79	featureless
J163716.73+131438.7	0.655	1.19	0.40	O II	6170	e	900 ± 100	-0.8 ± 0.2
				Ca II	6523	g	1100 ± 100	$+0.7 \pm 0.07$
				Ca II	6566	g	800 ± 300	$+0.4 \pm 0.09$
				G band	7124	g	800 ± 200	$+0.8 \pm 0.2$
J214406.27–002858.1	$0.34 < z \lesssim 2.5$	1.36	1.45	featureless
J224448.09–000619.3	0.640	0.88	0.35	Ca II	6450	g	1300 ± 100	$+0.75 \pm 0.05$
				Ca II	6511	g	1300 ± 300	$+0.7 \pm 0.1$
				G band	7057	g	1200 ± 300	$+0.55 \pm 0.07$
J224730.18+000006.4	$0.898 < z \lesssim 2.5$	1.27	0.52	Mg II	5311	a	1800 ± 100	$+3.0 \pm 0.1$

Note. — (a) Object ID. (b) Average redshift from the single lines or limits: lower limits from intervening systems or following Sbarufatti et al. (2005b) for featureless spectra; upper limits from absence of $Ly\alpha$ absorptions following Shaw et al. (2013) and references therein. (c) Spectral index of the continuum, defined by $F_\nu \propto \nu^{-\alpha_\nu}$. (d) Minimum detectable equivalent width (observer frame). (e) Line identification. (f) Wavelength at the center of the feature. (g) Type of feature: e: emission line; g: host galaxy absorption line; a: intervening system absorption line. (h) Full Width Half Maximum of the line. (i) Line equivalent width (observer frame).

Table 3: Fermi LAT detections for the target objects.

Source	in 2LAC	2 FGL name	R.A. [deg]	Dec. [deg]	error [deg]	$F_{0.1-100 \text{ GeV}}$ $\times 10^{-9}$ [ph cm $^{-2}$ s $^{-1}$]	Photon Index	TS	Time	$f_{0.1-100 \text{ GeV}}$ $\times 10^{-8}$ [ph cm $^{-2}$ s $^{-1}$]	Photon Index	TS_h
(a)		(b)	(c)	(c)	(d)	(e)	(f)	(g)	(h)	(i)	(j)	(k)
J003808.50+001336.5	Y	J0038.1+0015	9.542	0.265	0.217	1.6 ± 0.7	-1.78 ± 0.15	42	2009/10/09	1.80 ± 0.16	1.74 ± 0.04	24
J125032.58+021632.1	192.578	2.308	0.095	2.2 ± 1.1	-1.85 ± 0.17	35	2009/11/08	2.07 ± 0.54	1.93 ± 0.13	15
J135120.84+111453.0	Y	J1351.4+1115	207.867	11.256	0.110	$< 2 \text{ (} 5\sigma \text{)}$	2012/04/26	1.16 ± 0.84	1.63 ± 0.30	24
J144052.93+061016.1	Y	J1440.9+0611	220.248	6.189	0.099	9.6 ± 2.1	2.1 ± 0.1	148	2008/12/13	2.72 ± 1.3	1.93 ± 0.23	34
J145507.44+025040.2	$< 2 \text{ (} 5\sigma \text{)}$	
J163716.73+131438.8	249.37	13.20	0.12	$< 2 \text{ (} 5\sigma \text{)}$	2011/09/29	10.2 ± 4.4	3.69 ± 0.60	9
J214406.27-002858.1	$< 2 \text{ (} 5\sigma \text{)}$	
J224448.09-000619.3	$< 2 \text{ (} 5\sigma \text{)}$	
J224730.19+000006.4	Y	J2247.2-0002	341.811	-0.049	0.152	$< 2 \text{ (} 5\sigma \text{)}$	2012/07/25	1.99 ± 1.3	1.93 ± 0.30	16

Note. — (a) Object ID. (b) Fermi Gamma-ray LAT designation in 2-year catalog. (c) γ counterpart coordinates. (d) 95% error radius. (e): Integral photon flux in 0.1-100 GeV range. (f) Photon Index defined as $\nu F_\nu \propto \nu^{-\Gamma+2}$. (g) Test Statistic (Mattox et al. 1996). (h) Time of highest significance observation: measures derived from 30 days integration around the date (± 15 d) in column (h). (i) Highest significance photon flux. (j) Photon Index of highest significance observation. (k) Highest Test Statistic.

Fig. 1.— Spectra of the objects in the observer frame. *Top panel*: Flux density spectrum in Relative Units (R. U.); *Bottom panel*: Slightly smoothed normalized spectrum (3 pixel kernel). Telluric bands are flagged by \oplus , spectral lines are marked by line identifications, absorption features from interstellar medium of our galaxy are labeled by ISM, diffuse interstellar bands by DIB.

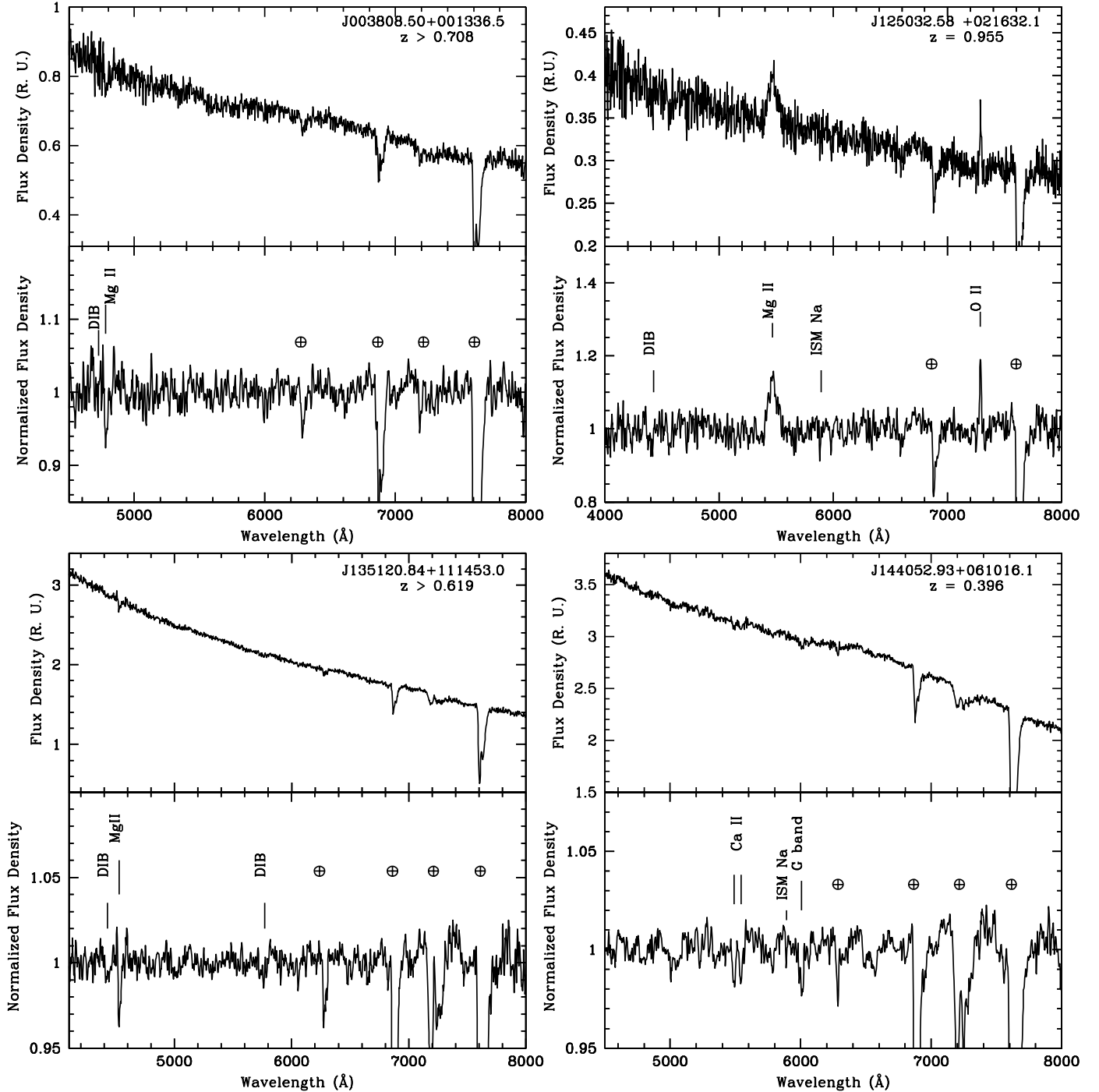


Fig. 1.— Continued

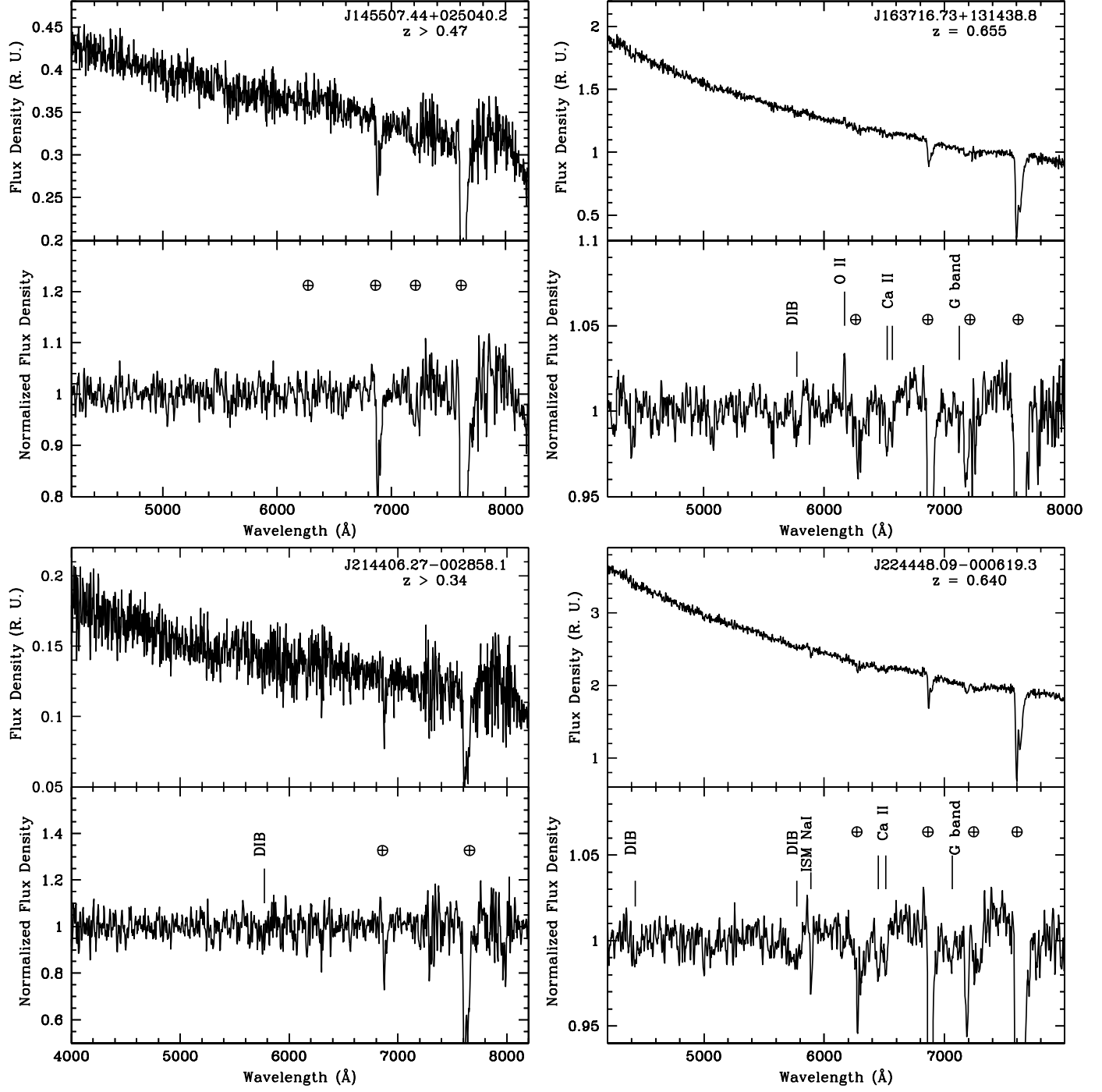
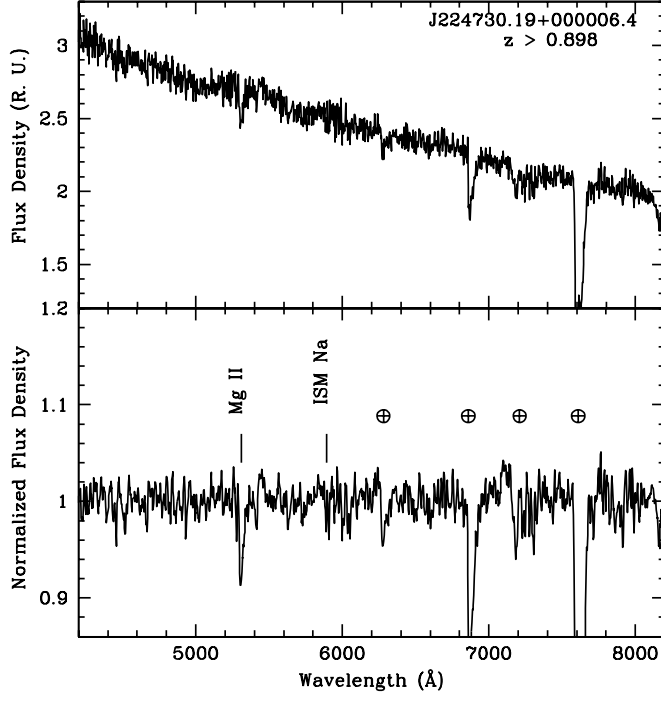


Fig. 1.— — Continued



REFERENCES

- Abazajian, K. N., Adelman-McCarthy, J. K., Agüeros, M. A., et al. 2009, *ApJS*, 182, 543
- Ackermann, M., Ajello, M., Allafort, A., et al. 2011, *ApJ*, 743, 171
- Ajello, M., Costamante, L., Sambruna, R. M., et al. 2009, *ApJ*, 699, 603
- Atwood, W. B., Abdo, A. A., Ackermann, M., et al. 2009, *ApJ*, 697, 1071
- Bade, N., Beckmann, V., Douglas, N. G., et al. 1998, *A&A*, 334, 459
- Becker, R. H., White, R. L., & Helfand, D. J. 1995, *ApJ*, 450, 559
- Beckmann, V., Engels, D., Bade, N., & Wucknitz, O. 2003, *A&A*, 401, 927
- Blandford, R. D., & Rees, M. J. 1978, *Phys. Scr*, 17, 265
- Caccianiga, A., Maccacaro, T., Wolter, A., Della Ceca, R., & Gioia, I. M. 2002, *ApJ*, 566, 181
- Carangelo, N., Falomo, R., Kotilainen, J., Treves, A., & Ulrich, M.-H. 2003, *High Energy Blazar Astronomy*, 299, 299
- Cardelli J. A., Clayton G. C., Mathis J. S., 1989, *ApJ*, 345, 245
- Collinge, M. J., Strauss, M. A., Hall, P. B., et al. 2005, *AJ*, 129, 2542
- Condon, J. J., Cotton, W. D., Greisen, E. W., et al. 1998, *AJ*, 115, 1693
- Croom, S. M., Smith, R. J., Boyle, B. J., et al. 2004, *MNRAS*, 349, 1397
- Danforth, C. W., Keeney, B. A., Stocke, J. T., Shull, J. M., & Yao, Y. 2010, *ApJ*, 720, 976
- Danforth, C. W., Nalewajko, K., France, K., & Keeney, B. A. 2013, *ApJ*, 764, 57

- Decarli, R., Dotti, M., & Treves, A. 2011, MNRAS, 413, 39
- Falomo, R., Maraschi, L., Treves, A., & Tanzi, E. G. 1987,a, Liege International Astrophysical Colloquia, 27, 153
- Falomo, R., Maraschi, L., Treves, A., & Tanzi, E. G. 1987,b, ApJ, 318, L39
- Falomo, R. 1990, ApJ, 353, 112005
- Farina, E. P., Decarli, R., Falomo, R., Treves, A., & Raiteri, C. M. 2012, MNRAS, 424, 393
- Giommi, P., Menna, M. T., & Padovani, P. 1999, MNRAS, 310, 465
- Giommi, P., Colafrancesco, S., Padovani, P., et al. 2009, A&A, 508, 107
- Giommi, P., Padovani, P., Polenta, G., et al. 2012, MNRAS, 420, 2899
- Green, R. F., Schmidt, M., & Liebert, J. 1986, ApJS, 61, 305
- Horan, D., & Wakely, S. 2008, AAS/High Energy Astrophysics Division #10, 10, #41.06
- Landoni, M., Falomo, R., Treves, A., et al. 2013, AJ, 145, 114
- Kimball, A. E., & Ivezić, Z. 2007, Bulletin of the American Astronomical Society, 39, #132.19
- Marcha, M. J. M., Browne, I. W. A., Impey, C. D., & Smith, P. S. 1996, MNRAS, 281, 42
- Mattox, J. R., Bertsch, D. L., Chiang, J., et al. 1996, ApJ, 461, 396
- Nolan, P. L., Abdo, A. A., Ackermann, M., et al. 2012, VizieR Online Data Catalog, 219, 90031
- Padovani, P., & Giommi, P. 1995, MNRAS, 277, 1477
- Padovani, P., Giommi, P., Landt, H., & Perlman, E. S. 2007, ApJ, 662, 182

- Plotkin, R. M., Anderson, S. F., Hall, P. B., et al. 2008, AJ, 135, 2453
- Plotkin, R. M., Anderson, S. F., Brandt, W. N., et al. 2010a, AJ, 139, 390
- Plotkin, R. M., Anderson, S. F., Brandt, W. N., et al. 2010b, ApJ, 721, 562
- Rector, T. A., Stocke, J. T., Perlman, E. S., Morris, S. L., & Gioia, I. M. 2000, AJ, 120, 1626
- Rector, T. A., & Stocke, J. T. 2001, AJ, 122, 565
- Sbarufatti, B., Treves, A., & Falomo, R. 2005,a, ApJ, 635, 173
- Sbarufatti, B., Treves, A., Falomo, R., et al. 2005,b, AJ, 129, 559 Paper I
- Sbarufatti, B., Treves, A., Falomo, R., et al. 2006,a, AJ, 132, 1 Paper II
- Sbarufatti, B., Falomo, R., Treves, A., & Kotilainen, J. 2006,b, A&A, 457, 35
- Sbarufatti, B., Ciprini, S., Kotilainen, J., et al. 2009, AJ, 137, 337
- Shaw, M. S., Romani, R. W., Cotter, G., et al. 2013, ApJ, 764, 135
- Schlegel D. J., Finkbeiner D. P., Davis M., 1998, ApJ, 500, 525
- Stickel, M., Padovani, P., Urry, C. M., Fried, J. W., & Kuehr, H. 1991, ApJ, 374, 431
- Stickel, M., Fried, J. W., & Kuehr, H. 1993, A&AS, 98, 393
- Stocke, J. T., Liebert, J., Schmidt, G., et al. 1985, ApJ, 298, 619
- Stocke, J. T., Morris, S. L., Gioia, I. M., et al. 1991, ApJS, 76, 813
- Stocke, J. T., Danforth, C. W., & Perlman, E. S. 2011, ApJ, 732, 113
- Tody D., 1986, SPIE, 627, 733

Veron, P. 1994, *A&A*, 283, 802

Voges, W., Aschenbach, B., Boller, T., et al. 1999, *A&A*, 349, 389

Ulrich M.H., 1989, in Maraschi, L., Maccacaro, T., & Ulrich, M.-H. 1989, *BL Lac Objects*, 334,

Wu, J., Brandt, W. N., Anderson, S. F., et al. 2012, *ApJ*, 747, 10